ARTICLE

Check for updates

Overexpression of KITLG predicts unfavorable clinical outcomes and promotes lymph node metastasis via the JAK/STAT pathway in nasopharyngeal carcinoma

Junjun Ling[1], Liang Zhang[1], Aoshuang Chang[1], Yi Huang[1], Jie Ren[1], Houyu Zhao[1 ✉] and Xianlu Zhuo [1 ✉]

Lymph node metastasis (LNM) is an early clinical sign and a contributor to the treatment failure in patients with nasopharyngeal carcinoma (NPC). The molecular mechanisms of LNM in NPC remain unclear. We aimed to identify and validate the possible key genes that play a crucial role in the LNM of NPC. The study included a discovery and validation phase. In the discovery phase, the key gene was identified by bioinformatics analysis. In the validation phase, the mRNA and protein expression of the key gene was detected by RT-PCR in NPC cells and by immunohistochemistry in a tissue microarray. Then, the effect of the key gene expression on cell invasion and migration was explored in vitro and in vivo. As a result, KITLG was identified as the key gene. The overexpression of KITLG was detected in NPC cells, which was correlated with neck lymph node metastasis and poor prognosis in patients with NPC. The suppression of KITLG inhibited the proliferation, invasion, and metastasis of NPC cells in vitro and in vivo. JAK/STAT signaling pathway might mediate the enhancement of cell invasion and metastasis caused by KITLG. In summary, the overexpression of KITLG in NPC cells might play a crucial role in the LNM of NPC, raising the possibility of KITLG as a prognostic factor and a potential target for NPC treatment.

INTRODUCTION

Nasopharyngeal carcinoma (NPC) is an epithelial carcinoma arising from the mucosal lining of the nasopharynx[1]. The annual incidence of NPC is ~30 per 100,000 persons[2]. The geographical global distribution of NPC is extremely unbalanced, and it is most prevalent in East and Southeast Asia, especially in southern China[3]. The ratio of the NPC incidence between males and females is ~2:5 in China[4]. Epidemiological studies suggest that active and passive tobacco smoking, consumption of alcohol and preserved foods, EBV infection, and host genetic variations are risk factors for NPC[5]. The pathogenesis of NPC is complicated. A good understanding of NPC pathogenesis may afford novel therapeutic interventions for its treatment.

The primary modality of treatment for NPC is radiotherapy. Considering the development of imaging, radiotherapy, and systemic treatment, NPC shows a favorable prognosis, with a 5-year overall survival (OS) rate of 75%[1]. Nevertheless, 30–40% of patients with NPC develop lymph node metastasis (LNM) or distant metastasis, which is an important cause of NPC-related death[6]. NPC is prone to metastasize to cervical lymph nodes. The incidence of cervical lymph node involvement reaches 85% in pathologically diagnosed NPC cases[7]. NPC can not only invade tissues adjacent to the nasopharynx but also develop distant metastasis to bone and organs such as the liver and lung via the vascular or lymphatic system[8]. Collectively, early LNM and distant metastasis account for 15–42% of treatment failures, which is a serious concern in NPC prevention and treatment[9].

The mechanism of LNM in NPC is complex and not fully understood. Multiple genes such as PTGS2, IRS-1, and CKS1, are involved in its biological processes[9–11]. However, these studies mainly concentrated on any certain gene/protein without considering that various aberrant genes/proteins might participate in the pathophysiological processes of LNM in NPC, and these genes/proteins interact with each other to form a network in this process[12]. Some genes/proteins that extensively interact with others might play an essential role in the biological processes of LNM, and they are recognized as hub genes[13,14]. The identification of these hub genes might help reveal the underlying mechanisms of LNM and determine effective approaches to the treatment of NPC.

In the present study, we aimed to identify and validate the key genes that may play a crucial role in the LNM of NPC. A discovery and validation phase was included in this study. In the discovery phase, we retrieved and analyzed the relevant data by using bioinformatics methods. The hub genes were identified, from which a key gene was filtered out. In the validation phase, the relationship of the key gene expression with clinical features was first evaluated in an NPC cohort assayed by immunohistochemistry (IHC). Then, further experiments were conducted to explore the effects of the key gene expression on the malignant abilities of NPC cells.

MATERIALS AND METHODS
Bioinformatics screening phase
The National Center for Biotechnology Information Gene Expression Omnibus (GEO) databases was retrieved, and the dataset GSE12452, which contains 31 NPC samples, was evaluated for investigating the critical genes

[1]Affiliated Hospital of Guizhou Medical University, Guiyang, China. ✉email: zhaohouyu@gmc.edu.cn; zhuoxianlu@gmc.edu.cn

involved in the LNM of NPC[15]. The dataset GSE12452 involved 41 samples (31 NPC and 10 normal tissues). Among the 31 NPC patients, 26 cases were accompanied by LNM, while the seven other cases were not. The differentially expressed genes (DEGs) between the NPC specimens with LNM and those without LNM were screened using GEO2R[16]. The genes that met the cutoff criteria of $P < 0.05$ and $\log_2$|fold change| of >1.0 were selected as the DEGs. Then, the DEGs were submitted to the STRING (https://string-db.org/) for the construction of protein–protein interaction (PPI) networks. A combined score of not <0.4 (median confidence score) was used as a threshold. Furthermore, the Cytoscape plug-in, Cytohubba, was used for ranking nodes in the PPI network[17]. The hub genes were identified in terms of the betweenness and degree values in the network. Venn analysis was performed on the top genes generated by different sorting methods. Then, the expression of genes from the intersection in NPC was evaluated in the Oncomine database[18], and the prognostic value was evaluated in the head and neck cancer cohort from the Cancer Genome Atlas (TCGA) database. Next, the key genes were identified for further research.

The possible functions of the DEGs were explored using the Panther tool[19] for evaluation. The pathway enrichment analysis was carried out.

Clinical specimens and cell lines
This study was approved by the ethics committee of the Institutional Ethics Review Board. Human NPC tissues (10 cases) and normal nasopharyngeal epithelial tissues (8 cases) were collected from the hospital. Informed consent was obtained prior to sample collection.

Human NPC cell lines, including 5-8F, S18, CNE2, HNE1, and 6–10B, and human immortalized nasopharyngeal epithelial cell line (NP69) were obtained from The Cell Bank of the Chinese Academy of Sciences (Shanghai, China). The samples were maintained in RPMI-1640 medium (Gibco, USA) supplemented with 10% fetal bovine serum (FBS, Gibco), 100 U/mL of penicillin (GIBCO), and 100 U/mL of streptomycin (GIBCO). All cell lines were incubated at 37 °C with 5% CO_2.

Generation of KITLG stable knockdown NPC cell lines
5-8F and S18 were plated in a 12-well plate at a concentration of 10^4 cells/ well. Lentivirus expressing short hairpin RNAs (shRNAs) targeting KITLG (sh-KITLG) and its control (sh-NC) were designed and built by GenePharma (Shanghai, China). Cells were transduced with this lentivirus for 24 h accompanied with polybrene (5 µg/ml). Puromycin (1 µg/ml) was used for 2–3 weeks to select KITLG stable knockdown cells.

Immunohistochemistry (IHC) staining and evaluation of KITLG
KITLG protein expression was tested using an NPC tissue chip that was obtained from the Outdo Biotech Co., Ltd. (Shanghai, China). The chip contained 129 cases of primary NPC samples. IHC staining was performed using the KITLG rabbit monoclonal antibody (anti-SCF, primary antibody; Abcam) according to the manufacturer's instructions.

The IHC results were evaluated and scored independently by two observers without knowledge of the clinical parameters of the cases in a blind manner. The IHC stain results were evaluated via integrated scoring was based on the intensity and percentage of positivity[20]. In brief, the staining intensity was scored from 0 to 3, where 0, 1, 2 and 3 represent negative, weak, moderate, and strong staining. The percentage of positivity was graded as follows: where 0 (0–5%), 1 (6–25%), 2 (26–50%), 3 (51–75%), and 4 (76–100%). The total IHC score was calculated as the product of staining intensity and percentage of positivity, with a range from 0 to 12, where 0–6 were classified as low expression, and >6 were classified as high expression.

CCK8 assay and colony formation assay
Cell proliferation was investigated by cell counting kit-8 assay (CCK-8; ImmunoWay Biotechnology Company Plano, TX, U.S.A.). We reseeded cells into a 96-well culture plate at a density of 4×10^3 in the logarithmic growth phase. The CCK8 reagent was added into the plates after culturing the cells in each group for 24, 48, 72, and 96 h, and the OD450 value was monitored. Furthermore, the clonogenic ability of NPC cells was detected using colony-forming assays. Cells were seeded into the six-well plate at a density of 600 per well. Crystal violet was used to stain the cells after incubation at 37 °C in a 5% humidified atmosphere for ~10 days, and the colonies were counted to assess the clonogenic ability of the cells.

Transwell migration and invasion assay
Transwell 24-well plates with 8-µm microporous filters (Corning, USA) were used to investigate the migration and invasion activity of NPC cells. The cells (5-8F and S18) were counted and resuspended in a serum-free medium. A total of 4×10^4 cells were seeded into the upper chambers, and they were coated with (invasion) or without (migration) Matrigel (BD, USA). The bottom chambers were filled with 600 µL of RPMI 1640 containing 20% FBS. The apparatus was incubated for 6 h at 37 °C for migration assay and 18 h at 37 °C for invasion assay. After incubation, cells in the inner wall of the chambers were removed, while cells in the lower filters (outside the chambers) were washed twice with PBS and stained with Giemsa (Sigma-Aldrich, St. Louis, MO) for 10 min. Lastly, images were obtained, and the number of the cells was counted.

Western blot assay
The cells were harvested and lysed in RIPA buffer (Beyotime, China) containing protease and phosphatase inhibitors. The protein qualification was determined using the BCA protein assay kit (Thermofisher, USA). Then, protein samples were separated by 10% SDS-PAGE gel. After electrophoresis, the proteins were transferred onto PVDF membranes (Bio-Rad, USA) in a running buffer with 20% methanol. After blocking with 5% bovine serum albumin (BSA), the blots were incubated at 4 °C overnight with the antibodies (Abcam, UK), which were diluted in TBST. The membranes were then incubated with horseradish peroxidase-conjugated secondary antibodies for 1 h at 37 °C in TBST. The protein bands were visualized using an ECL detection reagent (Beyotime, China).

Quantitative real-time polymerase chain reaction (qRT-PCR) assay
Total RNA was extracted from tissues or cells by TRIzol Reagent (Invitrogen, ThermoFisher Scientific, USA) and then reverse-transcribed to cDNA by using the PrimeScript RT reagent kit (TaKaRa, Japan) according to the manufacturer's instruction. The primer sequences were presented as follows[21]:

KITLG-forward: 5′-AGCCTTATACTGGAAGAAGAGAC-3′
KITLG-reverse: 5′-GTTGATACAAGCCACAATTACAC-3′
GAPDH- forward: 5′- GCTCTCTGCTCCTCCTGTTC-3′
GAPDH-reverse: 5′-CGACCAAATCCGTTGACTCC-3′
KIT-forward: 5′-CGTGGGCGACGAGATTAGG -3′
KIT-reverse: 5′-CTTCTTTCCCATACAAGGAGCG-3′
Each PCR amplification was performed in triplicate.

Animal experiment
All animal experimental protocols were carried out in accordance with the principles established by the Animal Care and Use Committee of our institute. Female BALB/c nude mice at 4–5 weeks of age were obtained from Charles River Laboratories (Beijing, China). The nude mice were divided randomly into two groups to receive inoculation of sh-KITLG cells or sh-NC cells.

For the nude mice xenograft model, sh-KTILG 5-8F, sh-KITLG S18, and control cells (2×10^5 cells in 30 µL serum-free DMEM) were subcutaneously injected. The measured tumor volume was plotted from the data measured every 5 days after an appearance and was calculated using the formula (length × width^2)/2. On day 28, all mice were euthanized, and the tumors were excised and weighed.

For the spontaneous lymphatic metastasis model, sh-KITLG 5-8F cells and the control (1×10^5 cells in 20 µL serum-free DMEM) were injected subcutaneously into the mouse footpads. The mice were sacrificed, and the popliteal lymph nodes from the hind limbs were harvested after 6 weeks.

Considering that HRPT has been used as a marker to distinguish metastatic and non-metastatic lymph node tissue[22], we also detected its expression in lymph nodes. Total RNA was extracted from the popliteal lymph nodes with TRIzol reagent. Approximately 1 µg of total RNA was used to synthesize cDNA, and 10 ng of cDNA was subjected to real-time PCR analysis for 40 cycles of amplification. Popliteal lymph nodes with a Ct value less than 30 were considered metastatic positive[23]. The primer of human HPRT forward: 5′-TTCCTTGGTCAGGCAGTATAATCC-3′; reverse: 5′-AGTCTGG CTTATATCCAACACTTCG-3′.

Assessment of the roles of KIT (c-kit) in NPC development and its relationship with KITLG

The KIT gene has been implicated as a cancer driver in many tumor types[24]. Considering that the KITLG gene product is the ligand for the KIT receptor (c-kit), we explored the expression and possible roles of c-kit in NPC cells and tissues.

The relationship between KIT and KITLG expression levels was evaluated by analyzing two external datasets from the GEO database (GSE40290 and GSE53819). GSE40290 contained 25 NPC samples and 8 normal controls, in which GSE53819 included 18 NPC samples and 18 normal controls.

The KIT mRNA in the cell lines was detected by qRT-PCR. The c-kit protein in NPC tissue was detected by IHC on the same NPC tissue chip, and that in the cell lines was assessed by Western blot analysis. The anti-c-kit and anti-p-c-kit antibodies (rabbit polyclonal, BIOSS) were used. Colony formation and transwell invasion assays were used to evaluate the malignant phenotype of cells.

Statistical analysis

Data in this study were analyzed using Graphpad Prism 7.0 software. The association between clinicopathological parameters and KITLG/c-kit protein expression levels was assessed using chi-squared test. For continuous variables, differences between the groups were analyzed using analysis of variance, t test or Wilcoxon rank sum test according to the concrete types of the data. OS was estimated using Kaplan–Meier survival analysis (log-rank test). $P < 0.05$ was considered statistically significant.

RESULTS

Screening of hub gene in the LNM of NPC by bioinformatics methods

Identification of DEGs from the selected gene expression profile. The GSE12452 dataset that was conducted on the GPL570 platform was retrieved from the GEO database and analyzed using the GEO2R tool. GSE12452 included 41 specimens, including 31 NPC cases. After comparing the NPC specimens with LNM and those without LNM, 70 upregulated and 14 downregulated genes were screened out. The top 10 up-/downregulated genes are shown in Table 1.

Table 1. Top 10 significant upregulated and downregulated DEGs between NPC patients with LNM and those without LNM.

Proble ID	Gene symbol	P value	logFC	Gene feature
214079_at	DHRS2	1.77E−04	2.22	Up
205680_at	MMP10	2.05E−02	2.12	Up
228547_at	NRXN1	5.15E−03	2.08	Up
204409_s_at	EIF1AY	4.57E−02	2.07	Up
214131_at	TXLNGY	4.85E−02	2.06	Up
230030_at	HS6ST2	6.55E−03	1.91	Up
205498_at	GHR	6.95E−03	1.85	Up
242881_x_at	DUXAP10	8.05E−03	1.68	Up
204455_at	DST	1.99E−02	1.66	Up
230760_at	ZFY	9.99E−03	1.62	Up
202345_s_at	FABP5	3.31E−02	−1.11	Down
203021_at	SLPI	4.90E−02	−1.25	Down
242915_at	ZNF682	1.10E−02	−1.28	Down
219607_s_at	MS4A4A	3.76E−03	−1.34	Down
229614_at	ZNF320	8.24E−03	−1.34	Down
209505_at	NR2F1	1.10E−02	−1.35	Down
221872_at	RARRES1	9.82E−03	−1.44	Down
221606_s_at	HMGN5	3.55E−03	−1.45	Down
228654_at	SPIN4	3.29E−03	−1.68	Down
235144_at	RASEF	4.09E−03	−1.73	Down

Pathway enrichment of DEGs. The results of KEGG pathway enrichment analysis indicate that the DEGs were enriched in 18 pathways, such as adenine and hypoxanthine salvage, JAK/STAT signaling, and apoptosis signaling pathway. The pathway terms are listed in Fig. 1A.

Hub gene screening through PPI network construction and Venn analysis. The PPI network was constructed using the STRING web tool, and the hub genes were identified using a plug-in of Cytoscape (Fig. 1B). The genes in the PPI network were ranked in terms of betweenness and degree. The top 5 genes ranked by degree (including MET, JAK2, KITLG, SGK1, and BMP2) and betweenness (including MET, JAK2, DNM3, KITLG, and GALNT3) are listed in Table 2. Venn analysis was performed to narrow the selection range of the hub genes (Fig. 1C). The results show that KITLG, MET, and JAK2 were included in the intersection, indicating that these genes may play an important role in the lymphatic metastasis of NPC.

mRNA expression of the hub genes evaluated in Oncomine. The expression levels of mRNA of KITLG, MET, and JAK2 were assessed in the Oncomine database. The Sengupta Head–Neck dataset that contains 10 nasopharynx and 31 NPC specimens was evaluated. The results are presented in Fig. 1D. The P values of SGK1, KITLG, and JAK2 were less than 0.05. Furthermore, compared with the normal control group, the mRNA expression levels of KITLG and JAK2 in NPC samples were significantly upregulated, while that of MET was significantly downregulated.

Prognostic value of the hub genes evaluated in TCGA. To assess the prognostic value of the hub genes, we evaluated the three hub genes in the head and neck carcinoma cohort from the TCGA. The gene expression levels were divided into a high and low expression group. The cutoff criteria for each group were set according to the median expression level of each gene. The relationship between the hub gene expression levels and the OS time was assessed using Kaplan–Meier survival. As shown in Fig. 1E, among the three hub genes, only KITLG affected the OS of patients. A high expression level of KITLG was associated with a poor prognosis for patients ($P < 0.05$). Therefore, KITLG was identified as the key gene and selected for further validation.

Validation of KITLG expression and prognostic value in NPC samples

KITLG mRNA was upregulated in NPC tissues and cell lines. First, we tested the mRNA expression level of KITLG in several NPC cell lines. As shown in Fig. 2A, the KITLG mRNA level was significantly higher than that in NP69 cells ($p < 0.05$), especially in 5-8F and S18 cells.

Next, we detected the relative mRNA expression of KITLG in 10 cases of NPC and 8 cases of normal nasopharyngeal epithelium. The results showed that the mRNA expression level of KITLG was significantly upregulated in NPC tissues relative to the normal controls ($p < 0.05$, Fig. 2B).

Protein expression of KITLG in an NPC cohort based on tissue microarray. To determine the association between KITLG protein expression and clinical features, we conducted IHC staining on a tissue microarray. A total of 129 NPC samples were observed on this slice. The clinical features of the 129 NPC cases are shown in Table 3. N-stage was unavailable in this cohort, but the status of neck LNM, the most frequent clinical finding of NPC, was included in the clinical features.

Specific staining was predominantly found in the cytoplasm of cancer cells (Fig. 2C). The IHC scores revealed that the expression level of KITLG was higher in NPC cases with LNM than that in NPC cases without LNM ($p < 0.01$, Fig. 2D).

According to the criteria for high and low expression mentioned above, the expression of KITLG was divided into two groups. As
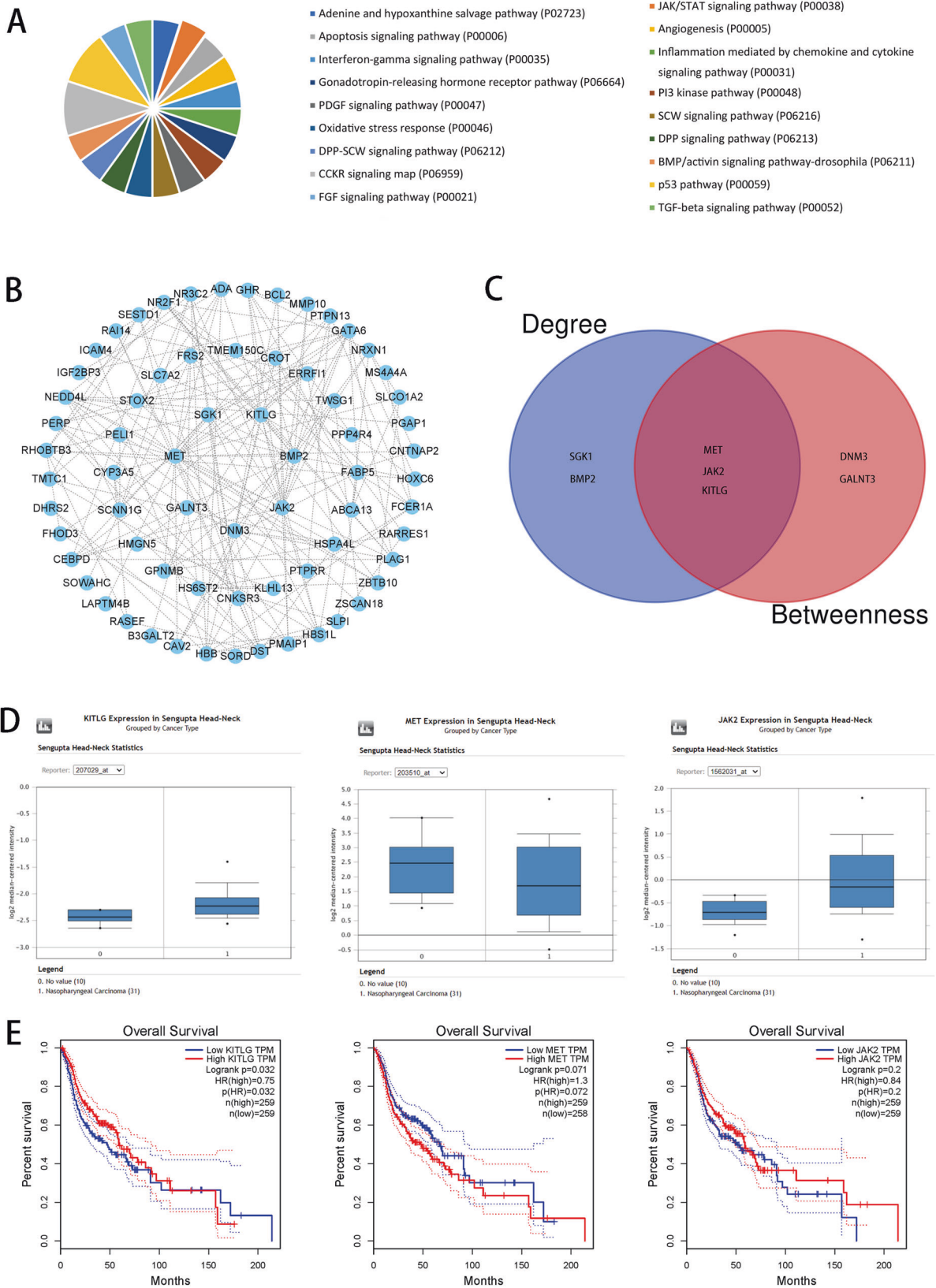
Fig. 1 Screening of hub genes related to the LNM of NPC. A Pathway enrichment analysis by Panther. **B** Protein–protein interaction network of the DEGs. **C** Screening of hub genes by Venn analysis. The intersection included three genes, namely, MET, JAK2, and KITLG. **D** The mRNA expression of MET, JAK2, and KITLG in NPC tissues (Oncomine). **E** The prognostic value of MET, JAK2, and KITLG in HNC (TCGA). Patients with high KITLG expression might have a shorter overall survival time than those with low KITLG expression (*P* < 0.05).

Table 2. Top 5 hub genes ranked by degree and betweenness values in the PPI network.

Gene symbol	Gene description	Degree	Betweenness
Sorted by degree			
MET	MET proto-oncogene, receptor tyrosine kinase	24	1154.939
JAK2	Janus kinase 2	18	482.4748
KITLG	KIT ligand	15	402.7323
SGK1	serum/glucocorticoid regulated kinase 1	13	306.0101
BMP2	bone morphogenetic protein 2	13	231.8265
Sorted by Betweenness			
MET	MET proto-oncogene, receptor tyrosine kinase	24	1154.939
JAK2	Janus kinase 2	18	482.4748
DNM3	dynamin 3	11	444.7778
KITLG	KIT ligand	15	402.7323
GALNT3	polypeptide N-acetylgalactosaminyltransferase 3	6	315.4389

depicted in Table 4, the association between KITLG expression levels and clinical features was determined. The data show that KITLG might have a positive correlation with recurrence ($p < 0.05$), presence of LNM ($p < 0.05$), and advanced clinical stage ($p < 0.05$).

Then, the association between KITLG protein expression and the prognosis of patients with NPC was evaluated. As depicted in Fig. 2E, patients with low KITLG expression had a higher survival probability than those with high KITLG expression ($p < 0.05$).

Knockdown of KITLG expression inhibits NPC cell proliferation in vitro and in vivo

The role of KITLG in NPC development was determined by subjecting the 5-8F and S18 cell lines to transfection of a plasmid containing shRNA targeting KITLG, and the samples were named as sh-KITLG-5-8F and sh-KITLG-S18, respectively. Cells stably transfected with empty plasmid were used as the controls and were named sh-NC-5-8F and sh-NC-S18. The expression of KITLG in these cells was validated by Western blot analysis. As shown in Fig. 3A, the expression of KITLG protein was significantly down-regulated in 5-8F and S18 cells with KITLG silencing (sh-KITLG-5-8F and sh-KITLG-S18).

CCK8 assay and colony formation assay were performed to assess the effects of KITLG on NPC cell proliferation in vitro. As depicted in Fig. 3B, compared with the sh-NC group, the cell proliferation was significantly decreased in the sh-KITLG group. Similarly, compared with the sh-NC group, the colony formation abilities were attenuated in the sh-KITLG-5-8F and sh-KITLG-S18 groups (Fig. 3C, D).

To further assess the effect of KITLG expression on cell proliferation in vivo, we subcutaneously injected the sh-KITLG-5-8F, sh-NC-5-8F, sh-KITLG-S18, and sh-NC-S18 cells into Balb/c nude mice ($n = 8$ per group). Consequently, the knockdown of KITLG expression remarkably inhibited the xenograft size and weight (Fig. 3E–G). The expression of KITLG protein was significantly lower in xenograft tumors formed by sh-KITLG-5-8F and sh-KITLG-S18 cells than that by sh-NC-5-8F and sh-NC-S18 cells, respectively (Fig. 3H). The results indicate that the downregulation of KITLG significantly inhibited the growth of NPC cells in vitro and in vivo.

KITLG affects NPC cell migration and invasion in vitro and in vivo

As shown in Fig. 4A–D, the migration/invasion abilities of sh-KITLG-5-8F and sh-KITLG-S18 were lower than those of sh-NC-5-8F and sh-NC-S18 cells, respectively, suggesting that KITLG expression could enhance the invasion/migration abilities of NPC cells.

To explore whether KITLG silence affects the lymphatic metastasis potential of the NPC cells in vivo, we constructed a lymphatic metastasis model by transplanting the sh-KITLG-5-8F

and sh-NC-5-8F cells into the footpads of Balb/c nude mice ($n = 30$ per group). After 6 weeks, the inguinal lymph nodes were dissected and analyzed. The results revealed that the volume and ratios of metastatic inguinal lymph nodes were significantly reduced in the sh-KITLG-5-8F group compared with the sh-NC-5-8F group ($P < 0.05$, Fig. 4E–H).

KITLG facilitates LNM via the JAK/STAT signaling pathway

The pathway enrichment analysis indicated that JAK/STAT signaling pathway (Fig. 1A) might be involved in the LNM process of NPC. Moreover, the MET and JAK2 were regarded as hub genes. This finding indicates that the JAK/STAT signaling pathway is correlated with KITLG expression.

In the present study, the expression of STAT3/p-STAT3 was also detected. The data showed that the ratios of the phosphorylated and total STAT3 in sh-KITLG-5-8F and sh-KITLG-S18 cells decreased relative to those in sh-NC-5-8F and sh-NC-S18 cells (Fig. 5A), suggesting that the STAT3 pathway activation might have a correlation with KITLG expression.

Colivelin is an activator of the JAK/STAT signaling pathway[25]. To further assess the role of STAT3 in the proliferation and aggressive tumor phenotype of NPC cells regulated by KITLG, Colivelin was used to activate STAT3 phosphorylation in KITLG-downregulation groups (sh-KITLG-5-8F and sh-KITLG-S18).

As shown in Fig. 5B–D, results of the CCK8 and colony formation assay show that the activation of the STAT pathway reversed the suppression of cell proliferation in sh-KITLG-5-8F and sh-KITLG-S18 cells, respectively. Consistently, the invasion and migration of sh-KITLG-5-8F and sh-KITLG-S18 cells were reversed by the use of Colivelin (Fig. 5E, F). Therefore, the JAK/STAT signaling pathway is involved in the promotion of cancer progression by KITLG.

Roles of KIT expression in NPC and its relationship with KITLG

By using GSE40290 and GSE53819 datasets, we found that KITLG was highly expressed in NPC tissues compared with the normal tissues ($P < 0.05$), but no significant difference was observed in KIT expression ($P > 0.05$). Correlation analysis showed no significant correlation between the expression levels of KIT and KITLG in NPC tissues ($P > 0.05$, Fig. 6A). IHC evaluation showed that the relationship between the expression levels of c-kit (KIT) and the clinical features was not significant (Table 5 and Fig. 6B). Moreover, the expression level of c-kit only slightly affected the OS time of patients with (Fig. 6C).

As shown in Fig. 6D, E, KIT mRNA and c-kit protein were not dysregulated in NPC cells relative to the controls ($P > 0.05$). Nevertheless, the phosphorylated c-kit (p-c-kit) was upregulated in NPC cells compared with the normal cells. Thus, an inhibitor of c-kit, AMG706 (Beyotime, China), was used to inhibit p-c-kit
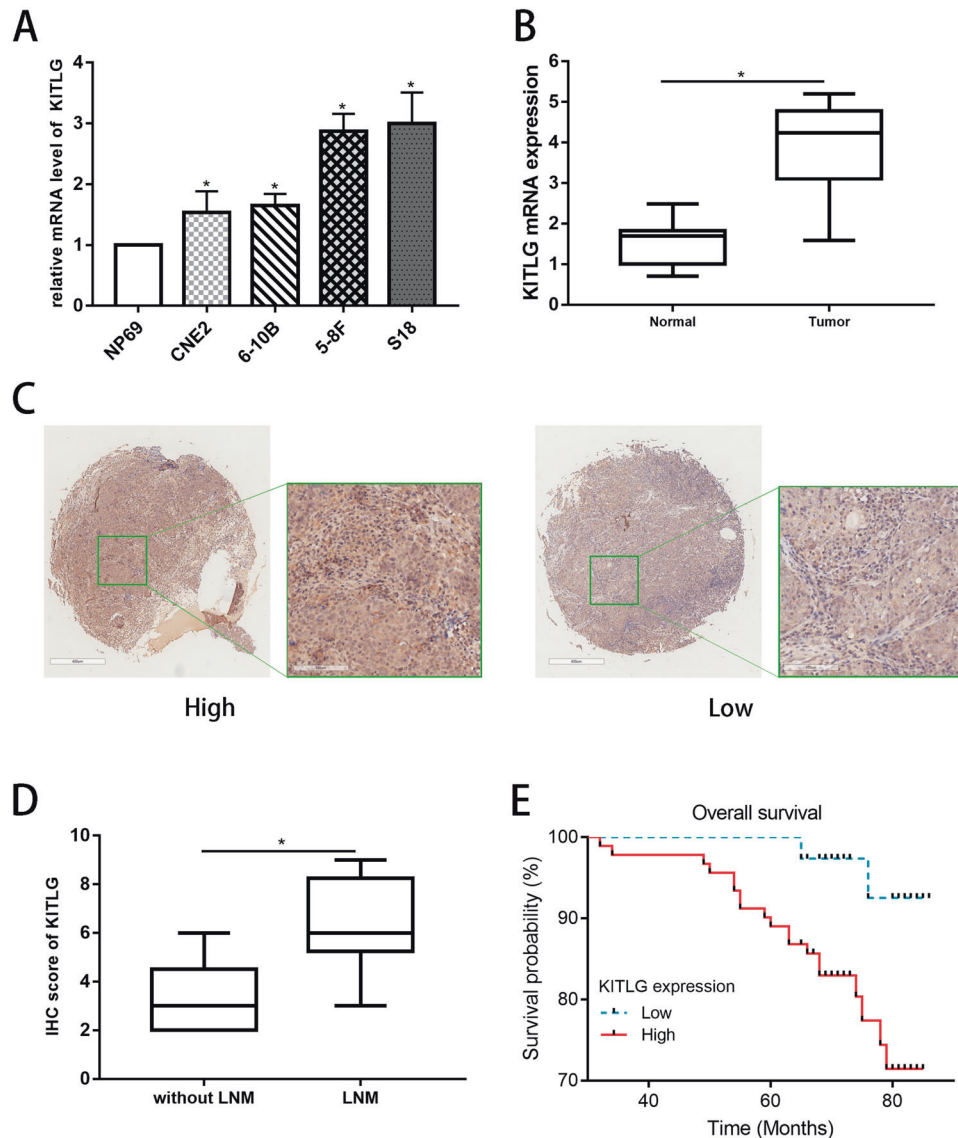
Fig. 2 Overexpression of KITLG in NPC is associated with neck LNM and poor prognosis. A Expression of KITLG mRNA in nasopharyngeal epithelial cell line NP69 and NPC cell lines (CNE2, 6–10B, 5-8F, and S18) as detected by qRT-PCR (*$p < 0.05$ vs. NP69, respectively). **B** Expression of KITLG mRNA in normal nasopharyngeal epithelial tissues ($n = 8$) and NPC tissues ($n = 39$) as detected by qRT-PCR (*$p < 0.05$). **C** Representative examples of KITLG expression in NPC tissues with high and low expression based on tissue microarray. **D** IHC score indicated that the KITLG expression in NPC patients with neck LNM was higher than that in patients without neck LNM ($p < 0.05$). **E** Survival curves showed that NPC patients with high expression of KITLG had a poor prognosis ($P < 0.05$).

expression. Based on literature[26], 15 nM AMG706 was used to treat cells for 48 h. The inhibition of c-kit weakened the cell proliferative and invasive abilities ($P < 0.05$, Fig. 6F, G).

DISCUSSION

LNM is an important contributor to the treatment failure in patients with NPC[27]. The mechanisms of LNM are complicated and remain unclear. In the present study, we have screened out a hub gene and further explored its roles in NPC. The results show that high KITLG expression might be an important contributor, and it could be associated with the enhanced migratory and invasive abilities of NPC cells.

This investigation included two phases, namely, the discovery and validation phase. In the discovery phase, we screened the DEGs associated with LNM by analyzing a gene expression profile retrieved from the GEO database. Through PPI network construction, KITLG was screened out to be a potential hub gene that was

associated with LNM in NPC. In the validation phases, KITLG was overexpressed in NPC specimens, which was positively correlated with LNM and a poor prognosis.

KITLG (KIT proto-oncogene ligand), a pleiotropic factor, is a ligand of the c-KIT tyrosine-kinase receptor, which is involved several biological processes, including tumorigenesis[28]. KITLG might play a role in multiple steps of tumor progression, while trials indicated that KITLG might be a diagnostic marker for thymoma[21]. Together with other genes, KITLG might be used as a prognostic signature for hepatocellular carcinoma[29]. In the present study, bioinformatics analysis showed that KITLG was overexpressed in NPC. IHC staining confirmed that the high expression of KITLG is correlated with advanced NPC stages and LNM. Laboratory experiments also indicated that KITLG might have a close association with the enhanced invasive and migratory abilities of NPC cells.

The mechanisms by which KITLG promotes cancer progression have not been clearly elucidated. A few studies have concerned

Table 3. Patient characteristics of the NPC cohort in the tissue microarray.

Characteristic	Total number of patients	Number of patients
Age (year)	129	
Median (range)		47 (20–82)
≥50		57
<50		72
Gender	129	
Male		99
Female		30
Recurrence	128	
Yes		59
No		69
Clinical stage	129	
1		15
2		55
3		39
4		20
Neck LNM	129	
With		93
Without		36

Table 4. Relationship between KITLG expression and clinicopathological paraments.

Variables	Total	KITLG expression		p value
		High (%)	Low	
Age				
≥50	57	38 (66.7)	19	0.611
<50	72	51 (70.8)	21	
Gender				
Male	99	71 (71.7)	28	0.224
Female	30	18 (60.0)	12	
Recurrence				
Yes	59	50 (84.7)	9	0.000
No	69	38 (55.1)	31	
Clinical stage				
1 + 2	70	37 (52.9)	33	0.000
3 + 4	59	52 (88.1)	7	
Neck LNM				
With	93	82 (88.2)	11	0.000
Without	36	7 (19.4)	29	
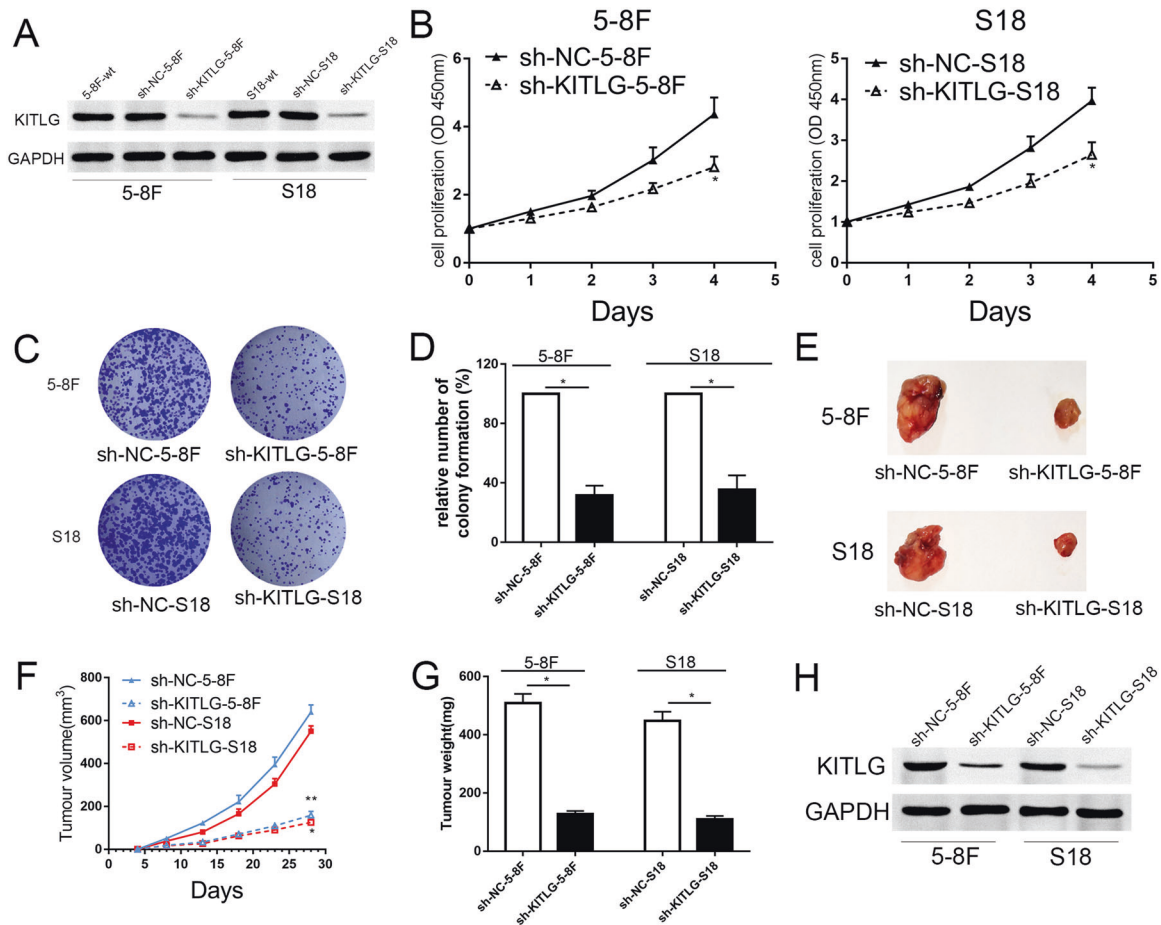
Fig. 3 KITLG promotes the proliferation of NPC cells in vitro and in vivo. A The expression level of KITLG protein decreased in sh-KITLG-5-8F/sh-KITLG-S18 compared with that in sh-NC-5-8F/sh-NC-S18 or 5-8-wt/S18-wt ($P < 0.05$). **B** CCK8 assays revealed that the cell proliferation of sh-KITLG-5-8F/sh-KITLG-S18 was significantly inhibited compared with sh-NC-5-8F/sh-NC-S18 (*$P < 0.05$). **C, D** The number of cell clones in sh-KTILG-5-8F/sh-KITLG-S18 was significantly lower than that in sh-NC-5-8F/sh-NC-S18 (*$P < 0.05$). **E** Resected tumor xenografts from each group. **F** Tumor volumes measured per 5 days of each group revealed that downregulation of KITLG remarkably suppressed tumor xenograft volumes (*$P < 0.05$ vs. sh-NC-S18; **$P < 0.05$ vs. sh-NC-5-8F). **G** Average weight of the excised tumors (28 days after inoculation; *$P < 0.05$). **H** KITLG protein expression in the excised tumors was analyzed by western blot analysis.
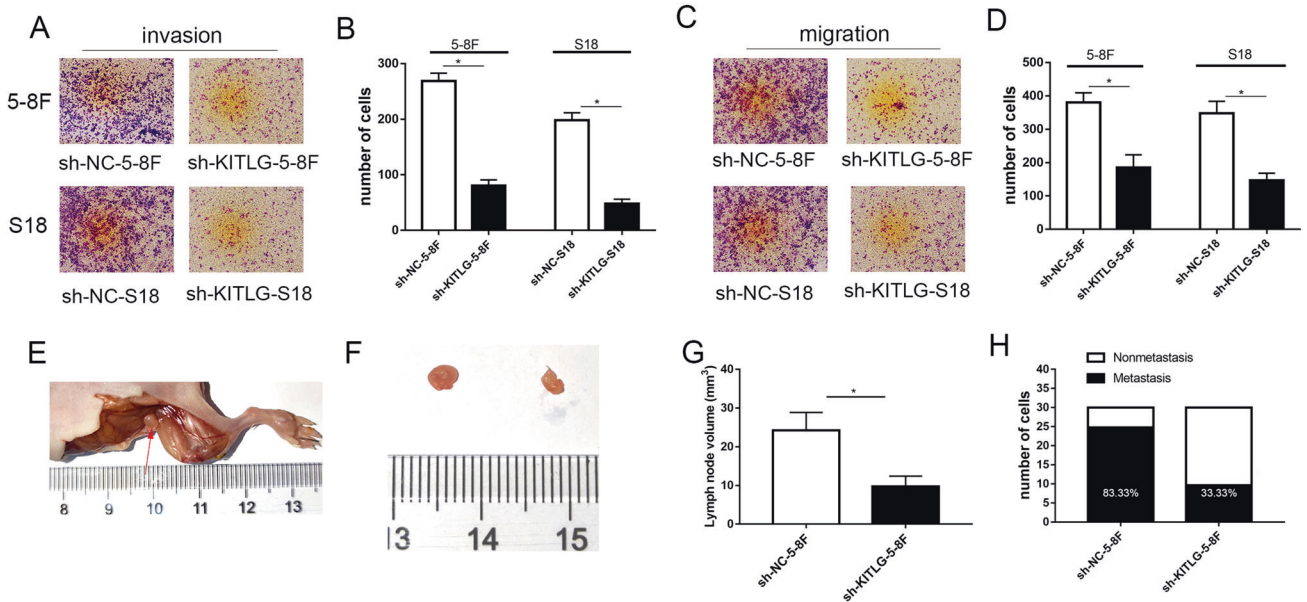
Fig. 4 KITLG affects the invasion and migration of NPC cells in vitro and in vivo. A, B Downregulation of KITLG reduced the invasion ability of 5-8F and S18 cells (*$P < 0.05$). **C, D** Downregulation of KITLG reduced the migration ability of 5-8F and S18 cells (*$P < 0.05$). **E, F** Inguinal metastatic lymph nodes removed from the lymphatic metastasis model. **G** The volume of the metastatic lymph nodes in Group sh-KITLG-5-8F was lower than that in Group sh-NC-5-8F ($P < 0.05$). **H** The rate of LNM in Group sh-KITLG-5-8F (33.3%) was lower than that in Group sh-NC-5-8F (83.3%).
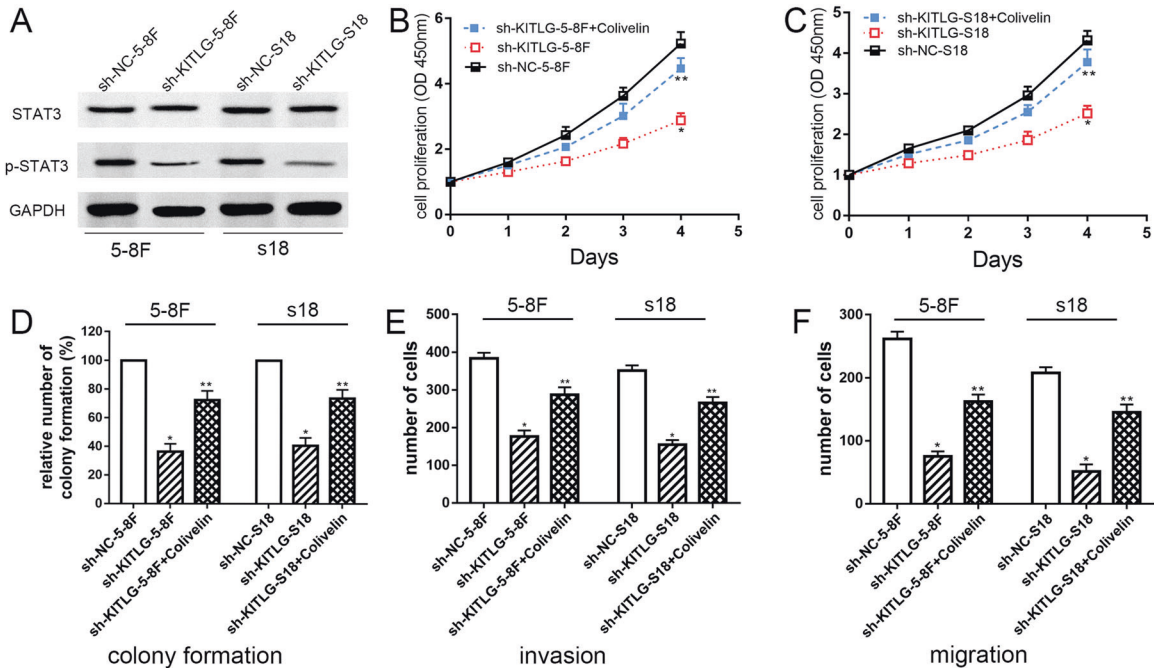

Fig. 5 KITLG facilitates LNM via the JAK/STAT signaling pathway. A The expression level of p-STAT3 was lower in sh-KITLG-5-8F (or sh-KITLG-S18) than that in sh-NC-5-8F (or sh-NC-S18, $P < 0.05$). **B, C** The cell proliferation of sh-KITLG-5-8F (or sh-KITLG-S18) decreased compared with that of sh-NC-5-8F (or sh-NC-S18), but the use of Colivelin resulted in an incomplete reversal (**B** *$P < 0.05$ vs. sh-KITLG-5-8F + Colivelin; **$P < 0.05$ vs. sh-KITLG-5-8F or sh-NC-5-8F; **C** *$P < 0.05$ vs. sh-KITLG-S18 + Colivelin; **$P < 0.05$ vs. sh-KITLG-S18 or sh-NC-S18). **D** Number of cell clones (*$P < 0.05$ vs. sh-NC group; **$P < 0.05$ vs. sh-NC group or sh-KITLG group). **E, F** The invasion and migration abilities of the cells in the three groups (*$P < 0.05$ vs. sh-NC group; **$P < 0.05$ vs. sh-NC group or sh-KITLG group).

this issue. For example, after miR-34c was used to silence the expression of KITLG, the cell proliferation, cell transformation, and invasive abilities of colon cancer cells were significantly inhibited[30]. In glioma cells, KITLG is correlated with the stemness property[31]. In addition, KITLG could be related to the recruitment of mast cells in breast cancer, which might facilitate cancer progression[32]. In the present study, the pathway enrichment analysis showed that the LNM-related DEGs were enriched in JAK/STAT pathway. Thus, we tested whether JAK/STAT pathway participate in the KITLG-mediated invasive abilities. The data
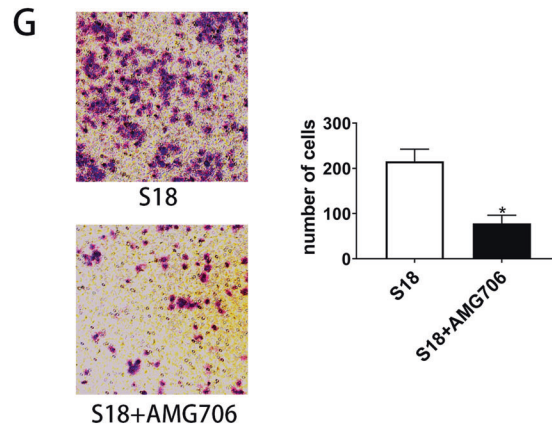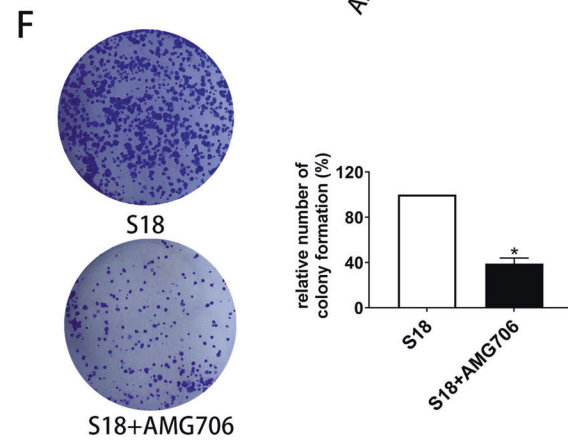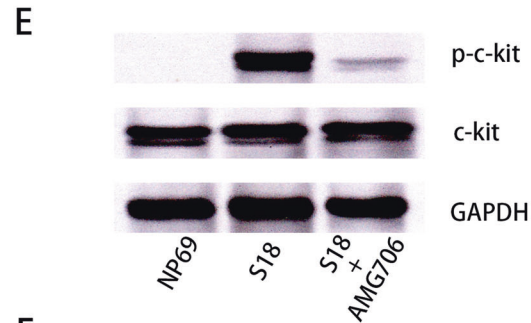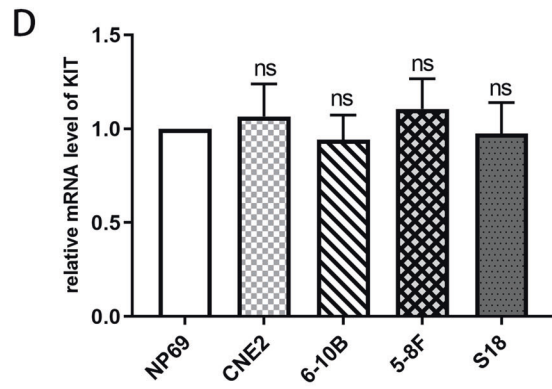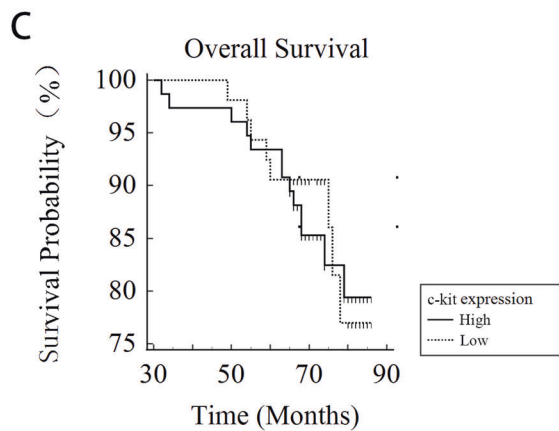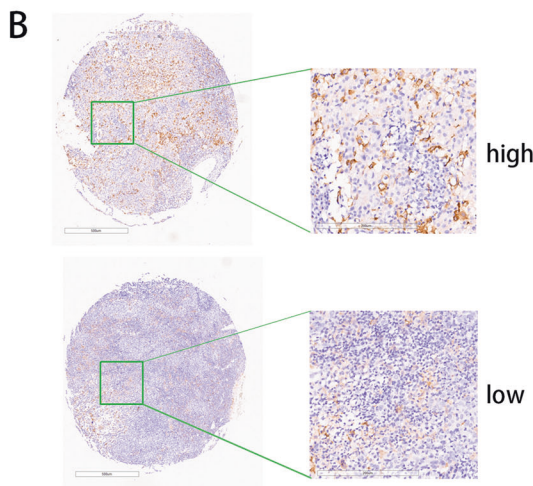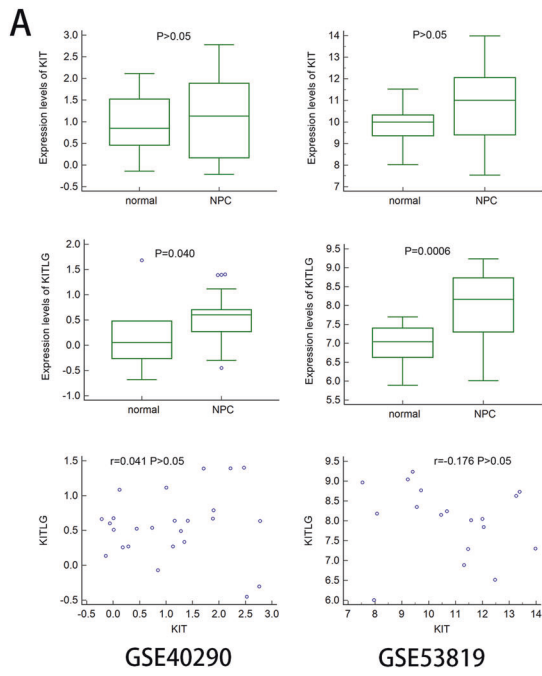
indicated that STAT activation might be a downstream event in KITLG-mediated invasion and metastasis of NPC cells. This finding is consistent with published studies. For example, the activation of STAT may be an essential event for the LNM in cervical cancer[33].

While in colorectal cancer, JAK/STAT could mediate the enhanced migration capabilities caused by a circRNA[34]. Thus, the activation of JAK/STAT acts as a survival factor in most cancers and could be a potential target for cancer therapy[35]. The present study

Fig. 6 Roles of KIT and its relationship with KITLG in NPC. A The NPC cohorts from GSE40290 and GSE53819 were used for validation. The expression of KITLG ($P < 0.05$) but not KIT ($P > 0.05$) was upregulated in NPC tissues relative to the normal controls. The association between KITLG and KIT expression in NPC tissues was not significant ($P > 0.05$). **B** The expression of c-kit in NPC tissues assessed by IHC. **C** The survival curve indicated that the expression levels of c-kit in NPC tissues slightly affected the overall survival ($P > 0.05$). **D** The expression of KIT mRNA in the cell lines. **E** The expression of c-kit and p-c-kit protein assessed by western blot assay. The use of AMG706 seemed to inhibit p-c-kit expression in S18 cells. **F** Colony formation assay showed that inhibition of p-c-kit resulted in decreased cell proliferation in NPC cells (*$P < 0.05$). **G** Transwell invasive assay showed that inhibition of p-c-kit resulted in weakened cell invasive abilities in NPC cells (*$P < 0.05$).

Table 5. Relationship between c-kit (KIT) expression and clinicopathological paraments.

Variables	Total	c-kit expression		p value
		High (%)	Low	
Age				
≥50	57	31 (54.4)	26	0.352
<50	72	45 (62.5)	27	
Gender				
Male	99	58 (58.6)	41	0.890
Female	30	18 (60)	12	
Recurrence				
Yes	59	36 (61.0)	23	0.607
No	69	39 (56.5)	30	
Clinical stage				
1 + 2	70	43 (61.4)	27	0.527
3 + 4	59	33 (55.9)	26	
Neck LNM				
With	93	54 (58.1)	39	0.752
Without	36	22 (61.1)	14	

demonstrated the importance of the JAK/STAT pathway in the LNM of NPC cells. In short, the aberrant expression of KITLG was observed in NPC cells, which promote cancer metastasis through the activation of the JAK/STAT pathway. However, the use of STAT activator could not completely reverse the inhibitory effect caused by KITLG suppression, possibly because in addition to JAK/STAT pathway, other pathways might be involved in this biological process.

KITLG, also known as stem cell factor, may interact with its receptor (KIT, or c-kit) and play various roles in different biological processes[36]. Thus, we also tested the roles of KIT in NPC cells. The results indicated that both KIT mRNA and c-kit protein were not dysregulated in NPC cells relative to the controls. The expression of KIT was not correlated with KITLG expression in NPC tissues. Unlike KITLG, the expression of c-kit protein had no significant effect on the prognosis of NPC patients. Binding to KIT receptor allowed KITLG to play its biological function. KITLG may also exert biological activity in many different aspects and pathways. However, phosphorylated c-kit plays an important role in the malignant progression of NPC cells, which requires further study.

Notably, several studies have concerned the effects of KITLG genetic variations on risks of diseases, particularly carcinoma. A family study showed that mutations of KITLG could increase melanoma and pharyngeal carcinoma risk[37]. However, the correlation between KITLG polymorphism and breast cancer risk has not been supported[38]. Similarly, a meta-analysis also failed to indicate an association between KITLG polymorphisms and testicular germ cell tumor risk[39]. Therefore, the results remain completely inconsistent, and future investigations are needed to address this topic.

Several limitations are involved in the present study. First, the sample sizes in both the discovery and validation phase were relatively limited, indicating the involvement of selection bias.

Future research with increased number of patients is necessary. In addition, several experimental approaches such as bioinformatics methods, IHC, and in vitro study were used for the investigation of KITLG. Nevertheless, the research on the mechanism is still superficial. Future studies should be conducted to further evaluate its functions in the LNM of NPC. Moreover, various investigations demonstrated that in addition to its expression, KITLG variations might also play important roles in the pathogenesis of multiple malignant tumors. Thus, the association between KITLG genetic variations and LNM should be explored in future studies. Additionally, several important genes such as JAK2, MET, and KITLG were in the same biological network. These genes may also interact with KITLG to promote the lymphatic metastasis of NPC cells. In future research, the interaction between these genes and KITLG should be examined in the process of LNM to provide new ideas for further mechanism mining.

In conclusion, KITLG is the key LNM-related gene for NPC. Our findings revealed the essential role of KITLG in promoting LNM in NPC. The data indicated that KITLG might not only act as a prognostic marker but also a potential therapeutic target in NPC.

DATA AVAILABILITY
The datasets used and/or analyzed during the current study are available from the corresponding author on reasonable request.

REFERENCES
1. Chen, Y.P., Chan, A.T.C., Le, Q.T., Blanchard, P., Sun, Y. & Ma, J. Nasopharyngeal carcinoma. *Lancet* **394**, 64–80 (2019).
2. Bray, F., Ferlay, J., Soerjomataram, I., Siegel, R.L., Torre, L.A. & Jemal, A. Global cancer statistics 2018: GLOBOCAN estimates of incidence and mortality worldwide for 36 cancers in 185 countries. *CA Cancer J Clin* **68**, 394–424 (2018).
3. Hong, M., Tang, K., Qian, J., Deng, H., Zeng, M., Zheng, S., et al. Immunotherapy for EBV-Associated Nasopharyngeal Carcinoma. *Crit Rev Oncog* **23**, 219–234 (2018).
4. Chen, W., Zheng, R., Baade, P.D., Zhang, S., Zeng, H., Bray, F., et al. Cancer statistics in China, 2015. *CA Cancer J Clin* **66**, 115–132 (2016).
5. Dai, W., Zheng, H., Cheung, A.K. & Lung, M.L. Genetic and epigenetic landscape of nasopharyngeal carcinoma. *Chin Clin Oncol* **5**, 16 (2016).
6. Yu, D., Han, G.H., Zhao, X., Liu, X., Xue, K., Wang, D., et al. MicroRNA-129-5p suppresses nasopharyngeal carcinoma lymphangiogenesis and lymph node metastasis by targeting ZIC2. *Cell Oncol (Dordr)* **43**, 249–261 (2020).
7. Ho, F.C., Tham, I.W., Earnest, A., Lee, K.M. & Lu, J.J. Patterns of regional lymph node metastasis of nasopharyngeal carcinoma: a meta-analysis of clinical evidence. *BMC Cancer* **12**, 98 (2012).
8. Chua, M.L.K., Wee, J.T.S., Hui, E.P. & Chan, A.T.C. Nasopharyngeal carcinoma. *Lancet* **387**, 1012–1024 (2016).
9. Yang, G., Deng, Q., Fan, W., Zhang, Z., Xu, P., Tang, S., et al. Cyclooxygenase-2 expression is positively associated with lymph node metastasis in nasopharyngeal carcinoma. *PLoS One* **12**, e0173641 (2017).
10. Chen, J.Y., Wu, X., Hong, C.Q., Chen, J., Wei, X.L., Zhou, L., et al. Downregulated ECRG4 is correlated with lymph node metastasis and predicts poor outcome for nasopharyngeal carcinoma patients. *Clin Transl Oncol* **19**, 84–90 (2017).
11. Xu, L., Fan, S., Zhao, J., Zhou, P., Chu, S., Luo, J., et al. Increased expression of Cks1 protein is associated with lymph node metastasis and poor prognosis in nasopharyngeal carcinoma. *Diagn Pathol* **12**, 2 (2017).
12. Teng, Y., Tao, X., Lu, W., Huang, Y., Xu, D., Li, M., et al. Identification of Hidradenitis Suppurativa-Related mRNA Expression Patterns Through Analysis of Gene Expression Omnibus. *Dose Response* **18**, 1559325820942646 (2020).
13. Xiang, Y., Zhang, L., Huang, Y., Ling, J. & Zhuo, W. Microarray-based data mining reveals key genes and potential therapeutic drugs for Cadmium-induced prostate cell malignant transformation. *Environ Toxicol Pharmacol* **68**, 141–147 (2019).

14. Zhang, L., Huang, Y., Yu, Z., Shao, M., Luo, Y. & Zhu, Y. Identification of key genes and pathways and therapeutic agents in cadmium-treated liver cells: A bioinformatics study. *Environ Toxicol Pharmacol* **56**, 145–150 (2017).

15. Dodd, L.E., Sengupta, S., Chen, I.H., den Boon, J.A., Cheng, Y.J., Westra, W., et al. Genes involved in DNA repair and nitrosamine metabolism and those located on chromosome 14q32 are dysregulated in nasopharyngeal carcinoma. *Cancer Epidemiol Biomarkers Prev* **15**, 2216–2225 (2006).

16. Barrett, T., Wilhite, S.E., Ledoux, P., Evangelista, C., Kim, I.F., Tomashevsky, M., et al. NCBI GEO: archive for functional genomics data sets–update. *Nucleic Acids Res* **41**, D991–995 (2013).

17. Chin, C.H., Chen, S.H., Wu, H.H., Ho, C.W., Ko, M.T. & Lin, C.Y. cytoHubba: identifying hub objects and sub-networks from complex interactome. *BMC Syst Biol* **8**, S11 (2014).

18. Rhodes, D.R., Yu, J., Shanker, K., Deshpande, N., Varambally, R., Ghosh, D., et al. ONCOMINE: a cancer microarray database and integrated data-mining platform. *Neoplasia* **6**, 1–6 (2004).

19. Mi, H., Ebert, D., Muruganujan, A., Mills, C., Albou, L.P., Mushayamaha, T., et al. PANTHER version 16: a revised family classification, tree-based classification tool, enhancer regions and extensive API. *Nucleic Acids Res* **49**, D394–D403 (2021).

20. Zhang, L., Huang, Y., Ling, J., Zhuo, W., Yu, Z., Luo, Y., et al. Overexpression of SLC7A11: a novel oncogene and an indicator of unfavorable prognosis for liver carcinoma. *Future Oncol* **14**, 927–936 (2018).

21. Yang, Z., Liu, S., Wang, Y., Chen, Y., Zhang, P., Liu, Y., et al. High expression of KITLG is a new hallmark activating the MAPK pathway in type A and AB thymoma. *Thorac Cancer* **11**, 1944–1954 (2020).

22. Tsaur, I., Renninger, M., Hennenlotter, J., Oppermann, E., Munz, M., Kuehs, U., et al. Reliable housekeeping gene combination for quantitative PCR of lymph nodes in patients with prostate cancer. *Anticancer Res* **33**, 5243–5248 (2013).

23. Qiang, Y.Y., Li, C.Z., Sun, R., Zheng, L.S., Peng, L.X., Yang, J.P., et al. Along with its favorable prognostic role, CLCA2 inhibits growth and metastasis of nasopharyngeal carcinoma cells via inhibition of FAK/ERK signaling. *J Exp Clin Cancer Res* **37**, 34 (2018).

24. Pathania, S., Pentikainen, O.T. & Singh, P.K. A holistic view on c-Kit in cancer: Structure, signaling, pathophysiology and its inhibitors. *Biochim Biophys Acta Rev Cancer* **1876**, 188631 (2021).

25. Zhao, H., Feng, Y., Wei, C., Li, Y., Ma, H., Wang, X., et al. Colivelin Rescues Ischemic Neuron and Axons Involving JAK/STAT3 Signaling Pathway. *Neuroscience* **416**, 198–206 (2019).

26. Kaya, T.T., Altun, A., Turgut, N.H., Ataseven, H. & Koyluoglu, G. Effects of a Multikinase Inhibitor Motesanib (AMG 706) Alone and Combined with the Selective DuP-697 COX-2 Inhibitor on Colorectal Cancer Cells. *Asian Pac J Cancer Prev* **17**, 1103–1110 (2016).

27. Lim, S.J., Iyer, N.G., Ooi, L.L., Koong, H.N., Chung, A.Y., Tan, H.K., et al. Metastasectomy for metachronous pulmonary and hepatic metastases from nasopharyngeal carcinoma: Report of 6 cases and review of the literature. *Head Neck* **38**, E37–40 (2016).

28. Pang, K., Hao, L., Shi, Z., Chen, B., Pang, H., Dong, Y., et al. Comprehensive gene expression analysis after ERH gene knockdown in human bladder cancer T24 cell lines. *Gene* **738**, 144475 (2020).

29. Yang, Y., Wu, G., Li, Q., Zheng, Y., Liu, M., Zhou, L., et al. Angiogenesis-Related Immune Signatures Correlate With Prognosis, Tumor Microenvironment, and Therapeutic Sensitivity in Hepatocellular Carcinoma. *Front Mol Biosci* **8**, 690206 (2021).

30. Yang, S., Li, W.S., Dong, F., Sun, H.M., Wu, B., Tan, J., et al. KITLG is a novel target of miR-34c that is associated with the inhibition of growth and invasion in colorectal cancer cells. *J Cell Mol Med* **18**, 2092–2102 (2014).

31. Aslam, N., Abusharieh, E., Abuarqoub, D., Ali, D., Al-Hattab, D., Wehaibi, S., et al. Anti-oncogenic activities exhibited by paracrine factors of MSCs can be mediated by modulation of KITLG and DKK1 genes in glioma SCs in vitro. *Mol Ther Oncolytics* **20**, 147–165 (2021).

32. Aponte-Lopez, A., Enciso, J., Munoz-Cruz, S. & Fuentes-Panana, E.M. An In Vitro Model of Mast Cell Recruitment and Activation by Breast Cancer Cells Supports Anti-Tumoral Responses. *Int J Mol Sci* **21** (2020).

33. Shi, S., Ma, H.Y. & Zhang, Z.G. Clinicopathological and prognostic value of STAT3/p-STAT3 in cervical cancer: A meta and bioinformatics analysis. *Pathol Res Pract* **227**, 153624 (2021).

34. Wang, J., Zhang, Y., Song, H., Yin, H., Jiang, T., Xu, Y., et al. The circular RNA circSPARC enhances the migration and proliferation of colorectal cancer by regulating the JAK/STAT pathway. *Mol Cancer* **20**, 81 (2021).

35. Tzeng, H.T., Chyuan, I.T. & Lai, J.H. Targeting the JAK-STAT pathway in autoimmune diseases and cancers: A focus on molecular mechanisms and therapeutic potential. *Biochem Pharmacol* **193**, 114760 (2021).

36. Mashayekhi, F., Shabani, S., Sasani, S.T. & Salehi, Z. The association of stem cell factor and soluble c-Kit (s-cKit) receptor serum concentrations with the severity and risk prediction of autism spectrum disorders. *Metab Brain Dis* **37**, 619–624 (2022).

37. Cuell, A., Bansal, N., Cole, T., Kaur, M.R., Lee, J., Loffeld, A., et al. Familial progressive hyper- and hypopigmentation and malignancy in two families with new mutations in KITLG. *Clin Exp Dermatol* **40**, 860–864 (2015).

38. Chen, W., Li, J., Liu, C., Chen, X., Zhu, Y., Yang, Y., et al. A functional p53 responsive polymorphism in KITLG, rs4590952, does not affect the risk of breast cancer. *Sci Rep* **4**, 6371 (2014).

39. Qin, J.X., Cai, Z.L., Yang, Y.F., Xing, J.C. & Zhuang, X. Association between KITLG Gene Polymorphisms and Testicular Germ Cell Tumors: A Systematic Review and Meta-analysis. *Curr Med Sci* **39**, 702–706 (2019).

AUTHOR CONTRIBUTIONS

Conception and study design: HZ, XZ. Conducted experiments: JL, LZ, AC, YH. Performed data analysis: JL, LZ, JR. Contributed to writing or critical assessment of the paper: JL, HZ, XZ.

COMPETING INTERESTS

The authors declare no competing interests.

ETHICS APPROVAL AND CONSENT TO PARTICIPATE

The authors state that they have obtained appropriate institutional review board approval or have followed the principles outlined in the Declaration of Helsinki for all human or animal experimental investigations. The present study used a commercial tissue microarray that was purchased from Shanghai Outdo Biotech Co., Ltd. and consent from the patients had been obtained.

ADDITIONAL INFORMATION

Supplementary information The online version contains supplementary material available at https://doi.org/10.1038/s41374-022-00817-4.

Correspondence and requests for materials should be addressed to Houyu Zhao or Xianlu Zhuo.

Reprints and permission information is available at http://www.nature.com/reprints

Publisher's note Springer Nature remains neutral with regard to jurisdictional claims in published maps and institutional affiliations.